# Liquid Crystalline Dendrimers Containing Photoactive Cinnamate Units

ANA I. VIÑUALES,[1] JOSE LUIS SERRANO,[2] RAQUEL GIMÉNEZ,[1] MILAGROS PIÑOL,[1] JAROSLAW TOMCZYK,[3] JOACHIM STUMPE[3]

[1]Química Orgánica, Facultad de Ciencias-Instituto de Ciencia de Materiales de Aragón, Universidad de Zaragoza-CSIC, Pedro Cerbuna, 12, 50009 Zaragoza, Spain

[2]Química Orgánica, Facultad de Ciencias-Instituto de Nanociencia de Aragón, Universidad de Zaragoza, Pedro Cerbuna, 12, 50009 Zaragoza, Spain

[3]Fraunhofer Institute for Applied Polymer Research, Geiselbergstrasse 69, 14476 Potsdam, Germany

Received 7 April 2011; accepted 20 May 2011
DOI: 10.1002/pola.24785
Published online 14 June 2011 in Wiley Online Library (wileyonlinelibrary.com).

**ABSTRACT**: Cinnamate-containing dendrimers have been prepared by peripheral functionalization of the amine groups of a poly(propyleneimine) dendrimer with 4-methoxycinnamate- or 4-(*N*,*N*-dimethylamino)cinnamate-derived units and/or 4-cyanobiphenyl units in different proportions. The synthesis, full characterization in solution, thermal properties and optical properties of the novel monomers, homodendrimers and codendrimers are reported. The composition of the molecular structure of the codendrimers has been elucidated by matrix assisted laser desorption/ionization time-of-flight mass spectrometry (MALDI-TOF MS). These liquid crystalline dendrimers display lamellar SmA mesophases. The codendrimers have been tailored in such a way that the photoactive units and the liquid crystal units absorb in different regions in order to allow better control over the processes induced by light. Linearly polarized UV light irradiation studies performed on thin films of the cinnamate codendrimers show that they are photoresponsive. A photoinduced anisotropy is generated with increasing exposure time, but in-plane amplification of anisotropy by thermal annealing in the mesophase was not observed. © 2011 Wiley Periodicals, Inc. J Polym Sci Part A: Polym Chem 49: 3499–3498, 2011

**KEYWORDS**: copolymerization; dendrimers; liquid crystal; MALDI; photoselection

**INTRODUCTION** Dendrimers are hyperbranched molecules that can be considered as intermediate between low molecular weight compounds and polymers. The defined chemical structures of these systems have unique characteristics depending on the type of nucleus, number and length of branches, and type of functional groups.[1,2] The possibility of designing dendrimers that are able to perform specific functions by chemical modification of their molecular structure has attracted enormous interest in many fields of science as they are seen as transport systems for biological or technological applications.[3–6] Among these properties, those concerning the controlled response to light have numerous potential applications due to the possibility of inducing macroscopically ordered materials by noncontact methods.[7,8]

Up to now, mainly photoactive side chain liquid crystalline polymers have been intensely investigated for this purpose. Among them, azobenzene or cinnamate polymers are able to generate films with high and stable photoinduced optical anisotropy based on axis-selective photoreactions that occur on irradiation with linearly polarized (LP) light, a process that leads to a self-organization in a preferred direction.[7,9–11] In some cases, the photoinduced anisotropy can be amplified significantly with subsequent thermal annealing in the mesophase.[12–15] This effect has been observed not only in homopolymers but in copolymers with small percentages (10–20 mol %) of photoactive units.[16–18]

As part of our work on functional polymers for optical applications, we were interested in transferring the concept outlined above to dendrimers by preparing novel liquid crystalline cinnamate-containing materials. Cinnamates are interesting photoactive units as they are able to yield angular-selective *E/Z* photoisomerization and [2+2] photocycloaddition processes. Side chain liquid crystalline cinnamate polymers have been shown to give good orientational properties under LPUV light irradiation,[13,14,19–21] and these materials are also more compatible with luminophores than azobenzene units,[22,23] thus allowing multifunctional properties in a single layer.[24] Furthermore, although some cinnamate dendrimers have been reported,[25,26] cinnamate liquid crystal (LC) dendrimers have barely been investigated.[27]

One of the possible strategies to obtain liquid crystalline properties with dendrimers involves the covalent modification of the periphery of a presynthesized dendritic core with liquid crystalline units.[28,29] In this work, we introduced liquid crystalline cyanobiphenyl-derived units and/or photoactive cinnamate-derived units into the third generation of poly(propyleneimine) (PPI) dendrimer, which contains 16 functionalizable terminal amino

Correspondence to: M. Piñol (E-mail: mpinol@unizar.es)

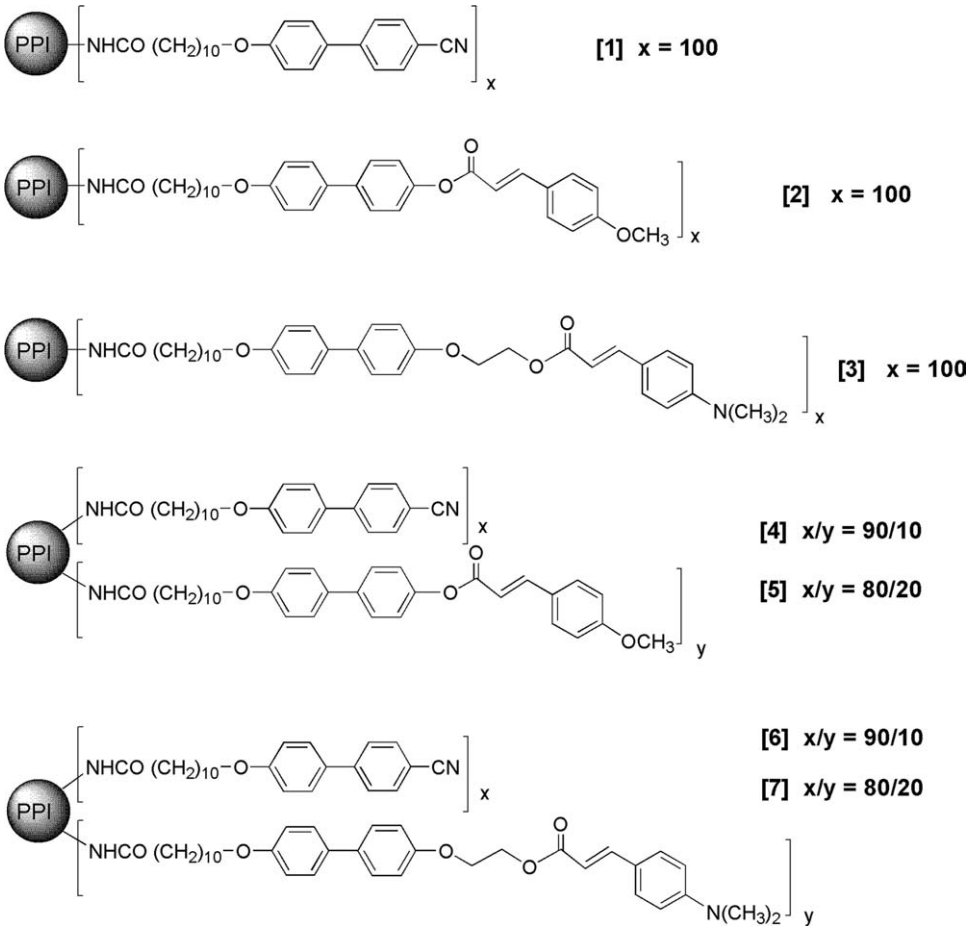


**FIGURE 1** Homodendrimers and codendrimers based on PPI-$(NH_2)_{16}$ ($x$ and $y$ represent the monomer feed in mol % and their sum equals 16).

groups. PPI dendrimers act as polar hyperbranched cores and these tend to stabilize liquid crystal phases by microsegregation.[30] In addition, it is expected that PPI systems will show lower transition temperatures than other polar dendritic cores such as poly(amido amine) (PAMAM) on peripheral functionalization with mesogenic units.[31] As photoactive units, we prepared two cinnamates with different optical properties. These systems are derived from 4-methoxycinnamate and 4-(*N,N*-dimethylamino)cinnamate (Fig. 1). These moieties were grafted onto the dendritic matrix through a flexible decamethylene spacer to decouple the matrix from the functional units in a similar way to photoactive side chain LC copolymers (Scheme 1).

In this work, we report the synthesis and characterization, as well as the thermal and optical properties, of the novel cinnamate promesogenic units and also the synthesis of homodendrimers and codendrimers which contain 80/20 and 90/10 mol %, respectively, of cyanobiphenyl/cinnamate units (Fig. 1). The compositions of the codendrimers were fully characterized by a combination of analytical techniques such as $^1$H NMR, UV–vis, and MALDI-TOF MS to gain structural information. The synthesis and full characterization of these molecules was a prerequisite to the study of their photoactive properties.

## EXPERIMENTAL

Dendrimers were prepared by an amidation reaction between the amine groups of PPI and pentafluorophenyl ester-terminated monomers (Scheme 1). Dendrimer [**1**] has been described previously.[30,32] The liquid crystalline unit pentafluorophenyl 11-[4′-cyano-4-biphenyloxy]undecanoate, denoted as **CNB**, was synthesized as reported.[30] The route for the novel pentafluorophenyl ester-terminated cinnamate monomers $\mathbf{M_{OMe}}$ and $\mathbf{M_{NMe2}}$ is shown in Scheme 2.

### Synthesis of the Monomers

#### *4′-Hydroxy-4-biphenyl 4-methoxycinnamate (P1)*

A solution of *N,N′*-dicyclohexylcarbodiimide (DCC) (22.5 g, 109 mmol) in DMF (75 mL) was added dropwise to a cold (0 °C) *N,N*-dimethylformamide (DMF) solution (250 mL) of 4,4′-dihydroxybiphenyl (20 g, 107 mmol), *N,N*-dimethyl-4-aminopyridine (DMAP) (1.31 g, 10.7 mmol), and 4-methoxycinnamic acid (17.2 g, 96 mmol). The mixture was stirred at r.t. for 3 days and filtered. The clear solution was diluted with water (300 mL) and extracted with dichloromethane (3 × 150 mL). The organic layer was dried, evaporated to dryness, and the residue was purified by column chromatography (silica gel, dichloromethane/ethyl acetate 9/1).

Yield: 13%. $^1$H NMR (300 MHz, $(CD_3)_2CO$, $\delta$, ppm): 8.48 (br s, 1H), 7.84 (d, $J = 15.9$ Hz, 1H), 7.75 (d, $J = 8.7$ Hz, 2H), 7.63 (d, $J = 8.9$ Hz, 2H), 7.52 (d, $J = 8.6$ Hz, 2H), 7.24 (d, $J = 8.6$ Hz, 2H), 7.04 (d, $J = 9.0$, 2H), 6.94 (d, $J = 8.6$ Hz, 2H), 6.64 (d, $J = 16.0$ Hz, 1H), 3.88 (s, 3H). IR (nujol, cm$^{-1}$): 3437–3353 (OH), 1728 (C=O), 1625 (C=C), 1591, 1549, 1509, 1493 (C-Car), 1257, 1214 (C—O).

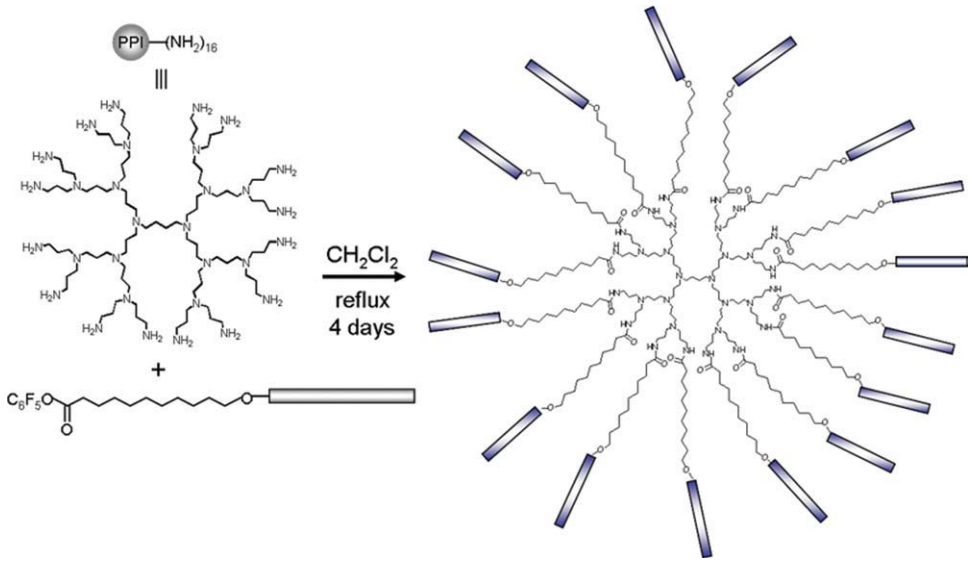


**SCHEME 1** Synthesis of the dendrimers.

***2-[4′-(Tetrahydropyranyl-2-oxy)-4-biphenyloxy] ethanol (P2)***

**Step 1.** 3,4-Dihydro-2*H*-pyran (DHP) (4.47 mL, 49 mmol) was added dropwise to a flask containing 4,4′-dihydroxybiphenyl (10 g, 54 mmol), *p*-toluensulfonic acid (PTSA) (0.46 g), and dry tetrahydrofuran (THF) (250 mL). The solution was stirred at r.t. for 2 h and evaporated to dryness. The solid was dissolved in diethyl ether and washed with an aqueous solution of NaOH (54 mmol) to remove most of the unreacted 4,4′-dihydroxybiphenyl. The organic layer was separated, dried over $MgSO_4$, and evaporated. The product, 4′-(tetrahydropyranyl-2-oxy)-4-hydroxybiphenyl, was purified by column chromatography (silica gel, hexane/ethyl acetate 10/1).

Yield: 37%. $^1$H NMR (300 MHz, $CDCl_3$, $\delta$, ppm): 7.41 (m, 4H), 7.07 (d, $J$ = 8.5 Hz, 2H), 6.85 (d, $J$ = 8.6 Hz, 2H), 5.43 (m, 1H), 4.79 (s, 1H), 4.00–3.86 (m, 1H), 3.65–3.56 (m, 1H), 2.10–1.50 (m, 6H). IR (nujol, cm$^{-1}$): 3350 (OH), 1609, 1592, 1499 (C-Car), 1266, 1229 (C—O), 1101, 827 (cyclic C—O—C).

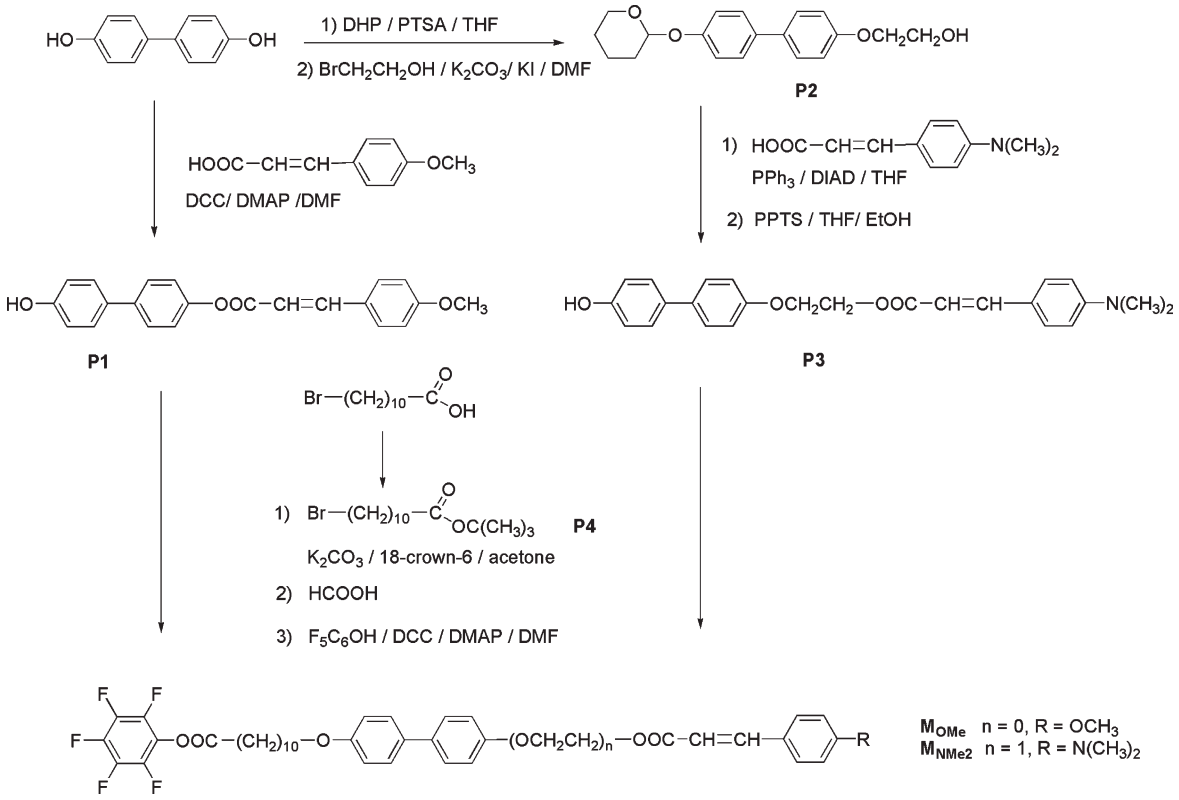


**SCHEME 2** Synthetic pathways followed for the preparation of the monomers.

**Step 2.** In Step 2, 2-bromoethanol (1.63 mL, 22 mmol) was added dropwise to a solution of 4′-(tetrahydropyranyl-2-oxy)-4-hydroxybiphenyl (5.40 g, 20 mmol), $K_2CO_3$ (4.15 g, 30 mmol), and KI (0.66 g, 4 mmol) in dry DMF (125 mL). The mixture was stirred at 140 °C for 24 h. After cooling, $H_2O$ (100 mL) was added, and the product was extracted with a mixture of hexane/ethyl acetate 1/2 (5 × 75 mL). The organic layer was washed with $H_2O$ (4 × 75 mL), dried, and evaporated to dryness. The resulting white solid was purified by washing the crushed solid in boiling hexane.

Yield: 79%. $^1$H NMR (300 MHz, $CDCl_3$, $\delta$, ppm): 7.47–7.42 (m, 4H), 7.08 (d, $J$ = 8.8 Hz, 2H), 6.95 (d, $J$ = 8.5 Hz, 2H), 5.44 (s, 1H), 4.20–4.05 (m, 2H), 4.06–3.85 (m, 3H), 3.70–3.57 (m, 1H), 2.15–1.80 (m, 3H), 1.79–1.50 (m, 4H). IR (nujol, cm$^{-1}$): 3452 (OH), 1606, 1498 (C-Car), 1267, 1238 (C—O), 1108, 813 (cyclic C—O—C).

### *2-(4′-Hydroxy-4-biphenyloxy)ethyl 4-(N,N-dimethylamino)-cinnamate (P3)*

**Step 1.** Triphenylphosphine (7.32 g, 27.9 mmol), 4-dimethylaminocinnamic acid (18.6 mmol), and dry dichloromethane (100 mL) were stirred for 30 min at r.t. **P2** (5.86 g, 18.6 mmol) and diisopropyl azodicarboxylate (DIAD) (5.48 mL, 27.9 mmol diluted in dry dichloromethane) were added. The mixture was stirred for 48 h and was evaporated to dryness. The residue was purified on a silica gel column (eluent hexane/ethyl acetate 8/2).

Yield of 2-[4′-(tetrahydropyranyl-2-oxy)-4-biphenyloxy]ethyl 4-(*N,N*-dimethylamino)cinnamate: 50%. $^1$H NMR (300 MHz, $CDCl_3$, $\delta$, ppm): 7.63 (d, $J$ = 16.2 Hz, 1H), 7.47–7.38 (m, 6H), 7.07 (d, $J$ = 8.9 Hz, 2H), 6.97 (d, $J$ = 8.8 Hz, 2H), 6.64 (d, $J$ = 8.7 Hz, 2H), 6.25 (d, $J$ = 15.9 Hz, 1H), 5.43 (t, $J$ = 3.1 Hz, 1H), 4.53 (t, $J$ = 4.9 Hz, 2H), 4.25 (t, $J$ = 4.6 Hz, 2H), 3.96–3.87 (m, 1H), 3.63–3.57 (m, 1H), 2.99 (s, 6H), 1.90–1.82 (m, 2H), 1.70–1.57 (m, 4H). IR (nujol, cm$^{-1}$): 1700 (C=O), 1626 (C=C), 1607, 1528, 1499 (C-Car), 1283,1240 (C—O), 1109, 818 (cyclic C—O—C).

**Step 2.** In Step 2, the product from Step 1 (3.98 mmol) and a mixture of THF (150 mL), ethanol (75 mL), and pyridinium *p*-toluensulfonate (PPTS) (1.02 g, 3.98 mmol) was stirred for 5 h at 50 °C and evaporated to dryness. The solid was dissolved in dichloromethane, and the solution was washed with $H_2O$ (4 × 75 mL), dried over $MgSO_4$, filtered, and evaporated to dryness. The solid was purified by washing the crushed solid with hexane.

Yield: 87%. $^1$H NMR (300 MHz, $CDCl_3$, $\delta$, ppm): 7.63 (d, $J$ = 15.9 Hz, 1H), 7.46–7.38 (m, 6H), 6.97 (d, $J$ = 9.1 Hz, 2H), 6.86 (d, $J$ = 8.5 Hz, 2H), 6.64 (d, $J$ = 9.0 Hz, 2H), 6.24 (d, $J$ = 15.9 Hz, 1H), 4.73 (s, 1H), 4.53 (t, $J$ = 4.6 Hz, 2H), 4.26 (t, $J$ = 4.7 Hz, 2H), 2.99 (s, 6H). IR (nujol, cm$^{-1}$): 3409 (OH), 1686 (C=O), 1604, 1528, 1499 (C-Car).

### *tert-Butyl 11-bromoundecanoate (P4)*

A solution of DCC (11.7 g, 57 mmol) in dry dichloromethane (40 mL) was added dropwise to a cold solution (0 °C) of 11-bromoundecanoic acid (15 g, 56 mmol), *tert*-butanol (5.9 mL, 62 mmol), and DMAP (0.68 g, 5.6 mmol) in dry dichloromethane (200 mL). The solution was stirred at r.t. for 3 days. The solid was filtered off, and the filtrate was washed with saturated aqueous $NaHCO_3$ (3 × 150 mL), dried over $MgSO_4$, filtered, and evaporated to dryness. The product was purified by column chromatography (silica gel, hexane/ethyl acetate 20/1).

Yield 31%. $^1$H NMR (300 MHz, $CDCl_3$, $\delta$, ppm): 3.38 (t, $J$ = 6.8 Hz, 2H), 2.18 (t, $J$ = 7.3 Hz, 2H), 1.86–1.78 (m, 2H), 1.58–1.52 (m, 2H), 1.42 (s, 9H), 1.27 (m, 12H). IR (neat, cm$^{-1}$): 1729 (C=O), 1252 (C—O).

### *4′-[10-(Pentafluorophenyloxycarbonyl)decyloxy]-4-biphenyl 4-methoxycinnamate ($M_{OMe}$)*

**Step 1.** A mixture of **P4** (3.6 g, 11.3 mmol), **P1** (3 g. 8.6 mmol), $K_2CO_3$ (2.15 g, 15.6 mmol), and 18-crown-6 ether (0.18 g, 0.7 mmol) in acetone (120 mL) was heated under reflux for 2 days. The mixture was evaporated to dryness and the residue was dissolved in hexane/ethyl acetate 1/2, washed with water (5 × 100 mL), dried, and evaporated to dryness. The resulting solid was purified by column chromatography (silica gel, hexane/ethyl acetate 9/1).

Yield of 4′-[10-(*tert*-butoxycarbonyl)decyloxy]-4-biphenyl 4-methoxycinnamate: 39%. $^1$H NMR (300 MHz, $CDCl_3$, $\delta$, ppm): 7.82 (d, $J$ = 15.9 Hz, 1H), 7.54 (d, $J$ = 8.5 Hz, 2H), 7.53 (d, $J$ = 8.8 Hz, 2H), 7.48 (d, $J$ = 8.4 Hz, 2H), 7.18 (d, $J$ = 8.7 Hz, 2H), 6.94 (d, $J$ = 8.4 Hz, 2H), 6.92 (d, $J$ = 8.8 Hz, 2H), 6.50 (d, $J$ = 15.9 Hz, 1H), 3.97 (t, $J$ = 6.5 Hz, 2H), 3.84 (s, 3H), 2.18 (t, $J$ = 7.3 Hz, 2H), 1.84–1.74 (m, 2H), 1.60–1.49 (m, 2H), 1.42 (s, 9H), 1.28 (s broad, 12H). IR (nujol, cm$^{-1}$): 1718 (C=O), 1627 (C=C), 1599, 1571, 1508, 1493 (C-Car), 1286, 1269, 1249, 1209 (C—O).

**Step 2.** The product from Step 1 (2.50 g, 4.7 mmol), formic acid (45 mL), and the minimum volume of dichloromethane to dissolve the solid were stirred at room temperature for 5 h. The mixture was evaporated to dryness, and the resulting solid was dissolved in hot ethyl acetate (300 mL). The solution was washed with $H_2O$ (5 × 200 mL), dried, and evaporated to dryness.

Yield of 4′-[10-(carboxy)decyloxy]-4-biphenyl 4-methoxycinnamate: 60%. $^1$H NMR (400 MHz, DMSO-$d_6$, $\delta$, ppm): 12.5–11.7 (m, 1H), 7.83 (d, $J$ = 15.9 Hz, 1H), 7.78 (d, $J$ = 8.5 Hz, 2H), 7.66 (d, $J$ = 8.6 Hz, 2H), 7.60 (d, $J$ = 8.8 Hz, 2H), 7.24 (d, $J$ = 8.6 Hz, 2H), 7.02 (d, $J$ = 8.9 Hz, 2H), 7.01 (d, $J$ = 8.8 Hz, 2H), 6.74 (d, $J$ = 15.9 Hz, 1H), 4.00 (t, $J$ = 6.4 Hz, 2H), 3.82 (s, 3H), 2.19 (t, $J$ = 7.3 Hz, 2H), 1.77–1.68 (m, 2H), 1.53–1.37 (m, 2H), 1.34–1.23 (s broad, 12H). IR (nujol, cm$^{-1}$): 3097–3010 (OH), 1719 (C=O), 1633 (C=C), 1604, 1598, 1573 (C-Car), 1287, 1256, 1223 (C—O).

**Step 3.** DCC (0.39 g, 1.9 mmol) dissolved in DMF (20 mL) was added dropwise to a cold solution (0 °C) of the acid obtained in the previous step (1 g, 1.9 mmol), pentafluorophenol (0.384 g, 2.1 mmol), and DMAP (0.023 g, 0.2 mmol) in DMF (65 mL). The reaction mixture was stirred for 3 days at r.t. The work-up was performed by adding $H_2O$ (80 mL), and the product was extracted with hexane/ethyl acetate 1/2 (4 × 100 mL). The organic layer was washed with water

(3 × 150 mL), dried over $MgSO_4$, filtered, and evaporated to dryness. The solid was purified by column chromatography (silica gel, dichloromethane as eluent).

Yield: 66%. $^1$H NMR (400 MHz, $CDCl_3$, $\delta$, ppm): 7.84 (d, $J$ = 16.0 Hz, 1H), 7.56 (d, $J$ = 8.9 Hz, 2H), 7.55 (d, $J$ = 9.0 Hz, 2H), 7.50 (d, $J$ = 8.9 Hz, 2H), 7.20 (d, $J$ = 8.7 Hz, 2H), 6.96 (d, $J$ = 8.9 Hz, 2H), 6.94 (d, $J$ = 8.8 Hz, 2H), 6.51 (d, $J$ = 15.9 Hz, 1H), 3.99 (t, $J$ = 6.6 Hz, 2H), 3.86 (s, 3H), 2.66 (t, $J$ = 7.4 Hz, 2H), 1.83–1.74 (m, 4H), 1.50–1.25 (m, 12H). $^{13}$C{$^1$H} NMR (100 MHz, $CDCl_3$, $\delta$, ppm): 169.6, 165.8, 161.7, 158.7, 149.8, 146.3, 143.0–136.0 (several broad and weak signals, $C_6F_5$), 138.5, 132.8, 130.0, 128.1, 127.7, 126.9, 121.8, 114.8, 114.6, 114.4, 68.0, 55.4, 33.3, 29.4, 29.3, 29.1, 28.8, 26.0, 24.7. $^{19}$F{$^1$H} NMR (282 MHz, $CDCl_3$, $\delta$, ppm): –152.79 (d, $J$ = 17.0 Hz, 2F), −158.20 (t, J = 21.3 Hz, 1F), −162.41 (dd, $J_1$ = 21.7 Hz, $J_2$ = 17.1 Hz, 2F). IR (KBr, cm$^{-1}$): 1786, 1727 (C=O), 1634 (C=C), 1602, 1573, 1518, 1495 (C-Car), 1288, 1252, 1216 (C—O). Anal. calcd for $C_{39}H_{37}O_6F_5$: C, 67.23; H, 5.35. Found: C, 67.57; H, 5.19. MS (FAB, $m/z$): 665 [M-$OCH_3$]$^+$.

### *2-[4′-[10-(Pentafluorophenyloxycarbonyl)decyloxy]-4-biphenyloxy]ethyl 4-(N,N-dimethylamino)cinnamate ($M_{NMe2}$)*

**Step 1.** A mixture of **P3** (2.27 g, 5.6 mmol), $K_2CO_3$ (1.20 g, 8.5 mmol), potassium iodide (KI) (0.187 mg, 1.1 mmol), dry DMF (80 mL), and **P4** (2 g, 6.2 mmol) was stirred at 90 °C for 24 h. The mixture was cooled to r.t., $H_2O$ (80 mL) was added and the solution was extracted with hexane/ethyl acetate 1/2 (4 × 100 mL). The organic layer was washed with water (4 × 200 mL), dried and evaporated to dryness. The product was purified by recrystallization from ethanol.

Yield: 98%. $^1$H NMR (400 MHz, $CDCl_3$, $\delta$, ppm): 7.65 (d, $J$ = 15.8 Hz, 1H), 7.47 (m, 4H), 7.42 (d, $J$ = 8.8 Hz, 2H), 6.99 (d, $J$ = 8.8 Hz, 2H), 6.94 (d, $J$ = 8.8 Hz, 2H), 6.66 (d, $J$ = 8.7 Hz, 2H), 6.27 (d, $J$ = 15.8 Hz, 1H), 4.56 (t, $J$ = 4.8 Hz, 2H), 4.28 (t, $J$ = 4.7 Hz, 2H), 3.98 (t, $J$ = 6.7 Hz, 2H), 3.02 (s, 6H), 2.20 (t, $J$ = 7.7 Hz, 2H), 1.84–1.74 (m, 2H), 1.60–1.55 (m, 2H), 1.44 (s, 9H), 1.37–1.29 (m, 12H). IR (nujol, cm$^{-1}$): 1725, 1698 (C=O), 1608, 1527, 1498 (C-Car), 1270, 1246, 1220 (C—O).

**Step 2.** This acid was obtained by a similar procedure to that reported for $\mathbf{M_{OMe}}$.

Yield of 2-[4′-[10-(carboxy)decyloxy]biphenyloxy]ethyl 4-(N,N-dimethylamino)cinnamate: 92%. $^1$H NMR (400 MHz, $CDCl_3$, $\delta$, ppm): 7.66 (d, $J$ = 15.6 Hz, 1H), 7.47 (m, 4H), 7.41 (d, $J$ = 8.5 Hz, 2H), 6.99 (d, $J$ = 8.6 Hz, 2H), 6.94 (d, $J$ = 8.4 Hz, 2H), 6.65 (d, $J$ = 8.5 Hz, 2H), 6.27 (d, $J$ = 15.9 Hz, 1H), 4.56 (t, $J$ = 4.5 Hz, 2H), 4.28 (t, $J$ = 4.5 Hz, 2H), 3.98 (t, $J$ = 6.5 Hz, 2H), 3.01 (s, 6H), 2.35 (t, $J$ = 7.7 Hz, 2H), 1.81–1.76 (m, 2H), 1.66–1.60 (m, 2H), 1.48–1.43 (m, 2H), 1.31 (m, 10H). IR (nujol, cm$^{-1}$): 3150–2923 (OH), 1710 (C=O), 1606, 1525, 1500 (C-Car), 1273, 1246 (C—O).

**Step 3.** The compound was obtained by a similar procedure to that reported for $\mathbf{M_{OMe}}$.

Yield: 64%. $^1$H NMR (400 MHz, $CDCl_3$, $\delta$, ppm): 7.66 (d, $J$ = 15.8 Hz, 1H), 7.47 (m, 4H), 7.42 (d, $J$ = 9.1 Hz, 2H), 6.99 (d, $J$ = 8.3 Hz, 2H), 6.95 (d, $J$ = 8.6 Hz, 2H); 6.66 (d, $J$ = 8.8 Hz, 2H), 6.27 (d, $J$ = 15.6 Hz, 1H), 4.56 (t, $J$ = 4.3 Hz, 2H); 4.28 (t, $J$ = 4.5 Hz, 2H), 3.99 (t, $J$ = 6.6 Hz, 2H), 3.02 (s, 6H), 2.66 (t, $J$ = 7.5 Hz, 2H), 1.84–1.73 (m, 4H), 1.51–1.31 (m, 12H). $^{13}$C{$^1$H} NMR (100 MHz, $CDCl_3$, $\delta$, ppm): 169.6, 167.8, 158.3, 157.7, 151.8, 145.9, 142.0–136.0 (several broad and weak signals, $C_6F_5$), 134.0, 133.2, 129.8, 127.7, 125.1 (broad, $C_6F_5$), 122.2, 115.0, 114.7, 111.8, 100.0, 68.1, 66.4, 62.6, 40.1, 33.3, 29.4, 29.3, 29.1, 28.8, 26.0, 24.8. $^{19}$F{$^1$H} NMR (282 MHz, $CDCl_3$, $\delta$, ppm): −152.79 (d, $J$ = 17.1 Hz, 2F), −158.19 (t, $J$ = 21.3 Hz, 1F), −162.41 (dd, $J_1$ = 17.0 Hz, $J_2$ = 21.4, 2F). IR (KBr, cm$^{-1}$): 1791, 1699 (C=O), 1609, 1521, 1499 (C-Car), 1271, 1248, 1223 (C—O). Anal. calcd for $C_{42}H_{44}F_5NO_6$: C, 66.95; H, 5.84; N, 1.86. Found: C, 66.75; H, 5.61; N, 1.95%. MS (FAB, $m/z$): 753 [M+H]$^+$.

## Synthesis of the Dendrimers

### *Dendrimer [2]*

To a solution of $\mathbf{M_{OMe}}$ (0.35 g, 0.5 mmol) in dry dichloromethane (20 mL), a solution of PPI-$(NH_2)_{16}$ (0.048 g, 0.028 mmol) was added dropwise in dichloromethane (2 mL). The mixture was heated under reflux for 3 days. The solid was filtered off, washed with dichloromethane and methanol, and dried in a vacuum oven at 90 °C for 12 h.

Yield: 90%. The compound is not soluble in common organic solvents which restricts its full characterization in solution. IR (KBr, cm$^{-1}$): 3295, 3074 (NH), 2925, 2850 ($CH_2$), 1724 (C=O),1631 (C=O, C=C), 1602, 1570, 1547, 1495 (C-Car), 1288, 1250, 1207 (C—O). Anal. calcd for $C_{616}H_{784}N_{30}O_{80}$: C, 74.82; H, 7.99; N, 4.25. Found: C, 74.16; H, 7.76; N, 5.01.

### *Dendrimer [3]*

To a solution of $\mathbf{M_{NMe2}}$ (0.5 g, 0.66 mmol) in dry dichloromethane (25 mL), a solution of PPI-$(NH_2)_{16}$ (0.063 g, 0.037 mmol) was added dropwise in dichloromethane (2 mL). The mixture was heated under reflux for 4 days. The mixture was diluted with dichloromethane, washed with saturated aqueous $Na_2CO_3$ (3 × 30 mL), dried, and evaporated to dryness. The resulting solid was purified by dissolving in dichloromethane and reprecipitation in hexane.

Yield: 58%. $^1$H NMR (400 MHz, $CDCl_3$, $\delta$, ppm): 7.64 (d, $J$ = 15.9 Hz, 16H), 7.46–7.38 (m, 96H), 7.17–7.11 (m, 16H), 6.95 (d, $J$ = 8.6 Hz, 32H), 6.90 (d, J = 8.5 Hz, 32H), 6.63 (d, $J$ = 8.9 Hz, 32H), 6.25 (d, $J$ = 15.6 Hz, 16H), 4.52 (t, $J$ = 4.6 Hz, 32H), 4.23 (t, $J$ = 4.6 Hz, 32H), 3.93 (t, $J$ = 6.4 Hz, 32H), 3.25–3.19 (m, 32H), 2.99 (s, 96H), 2.28–2.52 (m, 84H), 2.17 (t, $J$ = 7.6 Hz, 32H), 1.80–1.70 (m, 32H), 1.68–1.50 (m, 64H), 1.48–1.20 (m, 220H). $^{13}$C{$^1$H} NMR (100 MHz, $CDCl_3$, $\delta$, ppm): 173.9, 165.5, 157.7, 151.8, 154.9, 133.1, 129.9, 127.7, 122.1, 114.9, 114.7, 111.7, 68.0, 66.3, 62.5, 40.1, 36.6, 29.6, 29.5, 29.4, 29.3, 26.1, 25.9. IR (KBr, cm$^{-1}$): 3284, 3073 (NH), 2921, 2849 ($CH_2$), 1703 (C=O), 1637 (C=O, C=C), 1598, 1549, 1524, 1494 (C-Car), 1263, 1239 (C—O). Anal. calcd for $C_{664}H_{896}N_{46}O_{80}$: C, 73.83; H, 8.36; N, 5.96. Found: C, 72.46; H, 8.30; N, 5.38.

### *Dendrimer [4]*

To a solution containing $\mathbf{M_{CNB}}$ (0.23 g, 0.42 mmol) and $\mathbf{M_{OMe}}$ (0.033 g, 0.047 mmol) in dichloromethane (20 mL), a

solution of PPI-$(NH_2)_{16}$ (0.045 g, 0.027 mmol) was added dropwise in dichloromethane (2 mL). The mixture was heated under reflux for 4 days. The mixture was diluted with dichloromethane, washed with saturated aqueous $Na_2CO_3$ (3 × 30 mL), dried, and evaporated to dryness. The resulting solid was purified by dissolving in dichloromethane and precipitation in hexane. This reprecipitation must be repeated if free monomers are observed.

Yield: 66%. $^1$H NMR (400 MHz, $CDCl_3$, $\delta$, ppm): 7.85 (d, $J$ = 15.9 Hz, 2H), 7.67 (d, $J$ = 8.1 Hz, 28H), 7.62 (d, $J$ = 8.3 Hz, 28H), 7.57–7.46 (m, 36H), 7.19 (d, $J$ = 7.2 Hz, 4H), 7.14–7.04 (br m, 16H), 6.96–6.93 (d, $J$ = 8.7; m, 40H) Hz, 6.51 (d, $J$ = 15.9 Hz, 2H), 3.98 (br t, $J$ = 6.4 Hz, 32H), 3.88 (s, 6H), 3.31–3.25 (m, 32H), 2.43–2.33 (m, 84H), 2.20 (m, 32H), 1.82–1.30 (m, 316H). $^{13}$C{$^1$H} NMR (100 MHz, $CDCl_3$, $\delta$, ppm): 173.7, 165.8, 161.8, 159.7, 158.7, 146.4, 145.1, 132.5, 131.2, 130.1, 128.3, 127.6, 127.0, 121.9, 119.1, 115.0, 114.5, 110.0, 68.1, 55.4, 52.0, 51.3, 37.7, 36.6, 29.6, 29.2, 27.0, 26.0, 24.2, 22.6. IR (KBr, cm$^{-1}$): 3296, 3073 (NH), 2924, 2851 ($CH_2$), 2224 (C[tbond]N), 1728 (C=O), 1641 (C=O, C=C), 1603, 1549, 1526, 1495 (C-Car), 1290, 1251, 1211 (C—O). Anal. calcd for $C_{490}H_{658}N_{44}O_{38}$: C, 75.72; H, 8.53; N, 7.93. Found: C, 73.06; H, 8.47; N 7.90.

***Dendrimer [5]***

This codendrimer was prepared by a similar procedure as for [**4**] with $\mathbf{M_{CNB}}$ (0.25 g, 0.46 mmol), $\mathbf{M_{OMe}}$ (0.08 g, 0.115 mmol), and PPI-$(NH_2)_{16}$ (0.054 g, 0.032 mmol).

Yield: 67%. $^1$H NMR (400 MHz, $CDCl_3$, $\delta$, ppm): 7.83 (d, $J$ = 16.3 Hz, 3H), 7.64 (d, $J$ = 8.2 Hz, 26H), 7.61 (d, $J$ = 8.1 Hz, 26H), 7.55–7.44 (m, 38H), 7.19–7.12 (m, 28H), 6.96–6.90 (m, 38H), 6.50 (d, $J$ = 15.7 Hz, 3H), 3.95 (t, $J$ = 6.5 Hz, 32H), 3.85 (s, 9H), 2.50–2.25 (m, 84H), 2.18 (t, $J$ = 7.0 Hz, 32H), 1.82–1.15 (m, 316H) . $^{13}$C{$^1$H} NMR (100 MHz, $CDCl_3$, $\delta$, ppm): 173.7, 159.7, 145.2, 132.6, 130.1, 128.3, 127.6, 127.0, 121.9, 119.1, 115.0, 114.5, 110.1, 68.1, 55.4, 52.2, 51.4, 37.8, 36.7, 29.5, 29.3, 27.2, 26.1, 26.0. IR (KBr, cm$^{-1}$): 3296, 3073 (NH), 2923, 2851 ($CH_2$), 2225 (C[tbond]N), 1730 (C=O), 1641 (C=O, C=C), 1603, 1549, 1527, 1495 (C-Car), 1290, 1252, 1211 (C—O). Anal. calcd for $C_{499}H_{667}N_{43}O_{41}$: C, 75.64; H, 8.48; N, 7.60. Found: C, 75.05; H, 8.93; N, 8.05.

***Dendrimer [6]***

This codendrimer was prepared by a similar procedure as for [**4**] with $\mathbf{M_{CNB}}$ (0.6 g, 1.10 mmol), $\mathbf{M_{NMe2}}$ (0.092 g, 0.12 mmol), and PPI-$(NH_2)_{16}$ (0.118 g, 0.07 mmol).

Yield: 74%. $^1$H NMR (400 MHz, $CDCl_3$, $\delta$, ppm): 7.69–7.56 (m, 58H), 7.49 (d, $J$ = 8.5 Hz, 32H), 7.46–7.38 (m, 8H), 7.15–7.07 (br, 16H), 6.95 (d, $J$ = 8.5 Hz, 32H), 6.90 (d, $J$ = 8.6 Hz, 4H), 6.64 (d, $J$ = 8.6 Hz, 4H), 6.25 (d, $J$ = 15.8 Hz, 2H), 4.54 (m, 4H), 4.25 (m, 4H), 3.96 (t, $J$ = 6.4 Hz, 32H), 3.32–3.20 (m, 32H), 3.01 (s, 12H), 2.48–2.26 (m, 84H), 2.18 (t, $J$ = 7.6 Hz, 32H), 1.83–1.71 (m, 32H), 1.70–1.21 (284H). $^{13}$C{$^1$H} NMR (100 MHz, $CDCl_3$, $\delta$, ppm): 173.7, 165.5, 159.7, 157.7, 145.1, 132.5, 131.2, 129.8, 128.3, 127.6, 127.0, 119.0, 115.0, 114.7, 111.8, 110.0, 68.1, 52.1, 51.4, 40.0, 37.7, 36.6, 29.6, 29.5, 29.4, 29.2, 27.1, 26.0, 25.9. IR (KBr, cm$^{-1}$): 3230, 3074 (NH), 2923, 2850 ($CH_2$), 2224 (C[tbond]N), 1706 (C=O), 1641 (C=O, C=C), 1602, 1549, 1526, 1494 (C-Car), 1289, 1249 (C—O). Anal. calcd for $C_{496}H_{672}N_{46}O_{38}$: C, 75.53; H, 8.59; N, 8.17. Found: C, 74.96; H, 7.99; N, 7.96.

***Dendrimer [7]***

This codendrimer was prepared by a similar procedure as for [**4**] with $\mathbf{M_{CNB}}$ (0.6 g, 1.10 mmol), $\mathbf{M_{NMe2}}$ (0.207 g, 0.27 mmol), and PPI-$(NH_2)_{16}$ (0.131 g, 0.078 mmol).

Yield: 69%. $^1$H NMR (400 MHz, $CDCl_3$, $\delta$, ppm): 7.68–7.57 (m, 55H), 7.51 (d, $J$ = 8.4 Hz, 32H), 7.46–7.38 (m, 12H), 7.16–7.08 (m, 16H), 6.99–6.92 (m, 32H), 6.91 (d, $J$ = 8.5 Hz, 6H), 6.66 (d, $J$ = 8.9 Hz, 6H), 6.27 (d, $J$ = 15.9 Hz, 3H), 4.55 (t, $J$ = 4.8 Hz, 6H), 4.27 (t, $J$ = 4.8 Hz, 6H), 3.97 (t, $J$ = 6.4 Hz, 32H), 3.30–3.20 (m, 32H), 3.02 (s, 18H), 2.50–2.24 (m, 84H), 2.20 (t, $J$ = 7.7 Hz, 32H), 1.83–1.70 (m, 32H), 1.68–1.20 (284H). $^{13}$C{$^1$H} NMR (100 MHz, $CDCl_3$, $\delta$, ppm): 171.4, 165.4, 164.3, 157.4, 155.9, 155.3, 149.5, 143.6, 142.8, 131.4, 130.8, 130.5, 130.2, 128.8, 127.5, 125.9, 125.3, 124.6, 119.7, 116.7, 112.7, 112.3, 109.4, 108.7, 107.6, 65.7, 65.6, 63.9, 60.1, 59.9, 49.7, 49.0, 37.7, 35.4, 34.3, 27.3, 27.1, 26.9, 24.7, 23.7, 23.6. IR (KBr, cm$^{-1}$): 3300, 3076 (NH), 2923, 2851 ($CH_2$), 2224 (C[tbond]N), 1705 (C=O), 1641 (C=O, C=C), 1601, 1549, 1525, 1495 (C-Car), 1290, 1249 (C—O). Anal. calcd for $C_{508}H_{688}N_{46}O_{41}$: C, 75.37; H, 8.57; N, 7.96. Found: C, 74.55; H, 8.41; N, 7.69.

**Characterization Techniques**

Instrumentation for the molecular characterization of the monomers and dendrimers was similar to that reported previously.[32] Thin films were prepared by spin coating (Laurell, WS-400B-6TFM-LITE) on quartz glass substrates. The frequency of the rotation was 2000 rpm, and the time of rotation was 2 min. A dynamic method was used with 30 $\mu$L volume of solution. The concentration of the dendrimer was 10 mg mL$^{-1}$ in 1,1,2-trichloroethane or THF (HPLC grade). The film thickness was measured by a Dektak 150 profilometer (Veeco).

The anisotropy in the films was induced by irradiation with linearly polarized light of an Argon ($Ar^+$) laser (Coherent, Innova 90-4) at $\lambda$ = 364 nm with a power density of 10 mW cm$^{-2}$, a Mercury lamp with an interference filter for $\lambda$ = 365 nm equipped with a polarizer resulting in a power density of 6.3 mW cm$^{-2}$, or, alternatively, a Helium-Cadmium (He-Cd) laser (Kimmon Electronics) at $\lambda$ = 325 nm with a power density of 20 mW cm$^{-2}$.

The angular-dependent UV–vis absorbance spectra were measured using a diode array XDAP Spectrometer (Polytec) equipped with a polarizer. The spectra were measured every 5°. The dichroism was calculated from the angular-dependent absorbance spectra at 375 nm or at 310 nm that correspond to the absorption bands of 4-(*N,N*-dimethylamino)cinnamate and 4-methoxycinnamate units, respectively. The dichroism was calculated according to the following equation:

$$D = (A_{max} - A_{min})/(A_{max} + A_{min})$$

where $D$ is the dichroism at a defined wavelength, $A_{max}$ is the maximal, and $A_{min}$ the minimal absorbance values at the defined wavelength.

## RESULTS AND DISCUSSION

### Synthesis and Molecular Structure Characterization of the Monomers

Photoactive monomers $\mathbf{M_{OMe}}$ and $\mathbf{M_{NMe2}}$ possess a biphenyloxy group covalently joined, either directly or through an ethylene spacer, to the cinnamate moiety (Scheme 2). This extended cinnamate design is favorable for mesogenic rodlike behavior and has proven to exhibit large photoinduced anisotropy values in side chain polymers, as the photoproducts obtained on irradiation with light are more anisometric than those obtained without the biphenyloxy moiety.[33] The cinnamate moiety is substituted in the para-position with a methoxy group (in $\mathbf{M_{OMe}}$) or a *N,N*-dimethylamino group (in $\mathbf{M_{NMe2}}$). $\mathbf{M_{OMe}}$ does not have an ethylene spacer between the biphenyloxy and the cinnamate moiety, which yields a more rigid and favorable system for mesomorphic properties than $\mathbf{M_{NMe2}}$. The combination of a different substitution at the cinnamate group and the presence/absence of the ethylene spacer provide two monomers with different absorption properties.

For the synthesis of $\mathbf{M_{OMe}}$, 4,4′-dihydroxybiphenyl was monoesterified with 4-methoxycinnamic acid in the first step. In the case of $\mathbf{M_{NMe2}}$, it was necessary to monoprotect the 4,4′-dihydroxybiphenyl with tetrahydropyran before alkylation with 2-bromoethanol and esterification with 4-(*N,N*-dimethylamino)cinnamic acid. The decamethylenic spacer was introduced into the photoactive units at the end of the synthetic route by a Williamson reaction with *tert*-butyl 11-bromoundecanoate. The protection of the carboxylic acid as a *tert*-butyl ester allowed the subsequent deprotection under weakly acidic conditions without any interference from the cinnamate functional group. Finally, the carboxylic acids were transformed into their pentafluorophenyl esters. The monomers were characterized by elemental analysis, MS, FTIR, $^1$H NMR, $^{13}$C NMR, and $^{19}$F NMR, and the data are in accordance with the proposed structures.

The UV–vis absorption spectra in chloroform solutions ($10^{-5}$ M) show a band at 298 nm for the CNB monomer, a broad band centered at 317 nm for $\mathbf{M_{OMe}}$, and two bands at 263 and 367 nm for $\mathbf{M_{NMe2}}$—thus showing the bathochromic effect induced by the *N,N*-dimethylamino group. It can be observed that the three monomers absorb at different wavelengths. Therefore, these compounds could be influenced and studied separately in photoirradiation experiments performed on the codendrimers (Fig. 2).

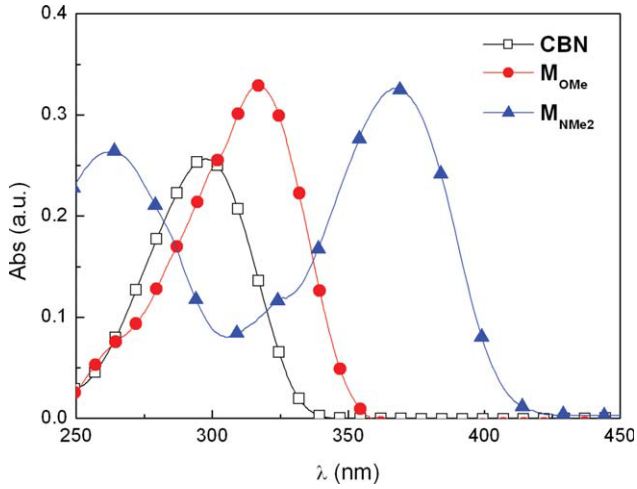


**FIGURE 2** UV–vis spectra of the monomers in chloroform solution. [Color figure can be viewed in the online issue, which is available at wileyonlinelibrary.com.]

### Synthesis and Molecular Structure Characterization of the Dendrimers

Dendrimers were synthesized by grafting the pentafluorophenyl ester monomers onto the periphery of the amine-terminated PPI core, with a molar feed ratio as outlined in Figure 1. The amidation reaction proceeded quantitatively as described for previous PPI functionalizations.[30,32,34,35] The third generation PPI was selected to avoid solubility problems associated with higher generations as low solubility would hinder the characterization and processability of the materials. The long decamethylenic spacer in the monomer helped to improve the solubility of the final materials compared to systems with shorter spacers. All of the dendrimers were soluble in common organic solvents except for [**2**], which precipitated out of the reaction medium as an insoluble solid. This drawback precluded all characterization of this material in solution.

All of the soluble dendrimers were characterized by elemental analysis, FTIR, $^1$H NMR, $^{13}$C NMR, gel permeation chromatography (GPC), MALDI-TOF, and UV–vis. In the FTIR spectra, N═H and C═O stretching bands corresponding to the amide group were observed. The compounds were free of precursor materials, as evidenced by the absence of N—H amine bands corresponding to PPI at 3370 cm$^{-1}$ or the C═O band from the pentafluorophenyl ester monomer at around 1790 cm$^{-1}$. For the cinnamate dendrimers, the C═C stretching band overlapped the amide band at 1640 cm$^{-1}$ in all cases. The C═O band of the cinnamic ester appears at 1729 cm$^{-1}$ for the 4-methoxycinnamate-derived dendrimers and at 1705 cm$^{-1}$ for the 4-(*N,N*-dimethyl)amino-derived dendrimers. The functionalization of the PPI dendrimer was confirmed by the presence of a broad singlet in the 6.5–7.2 ppm region (corresponding to the amide protons) in the $^1$H NMR spectra and a signal at 175 ppm due to the amide carbon in the $^{13}$C NMR spectra.

The $^1$H NMR spectra also proved useful in estimating the average compositions of the codendrimers. Proton resonances corresponding to the functional unit (**CNB** or cinnamate) were compared to determine the average relative concentration of each unit in a given codendrimer. The $^1$H NMR spectrum of dendrimer [**5**] is shown in Figure 3 and the values, which are in fair agreement with the theoretical ones, are shown in Table 1. For codendrimers [**6**] and [**7**], the different absorption regions of the two constitutive monomers, **CNB** and $\mathbf{M_{NMe2}}$, also allowed us to calculate the percentage composition by UV–vis spectroscopy, as the spectra of the dendrimers in solution were similar to the sum of the spectra of the separate monomers (Fig. 4 and Table 1).

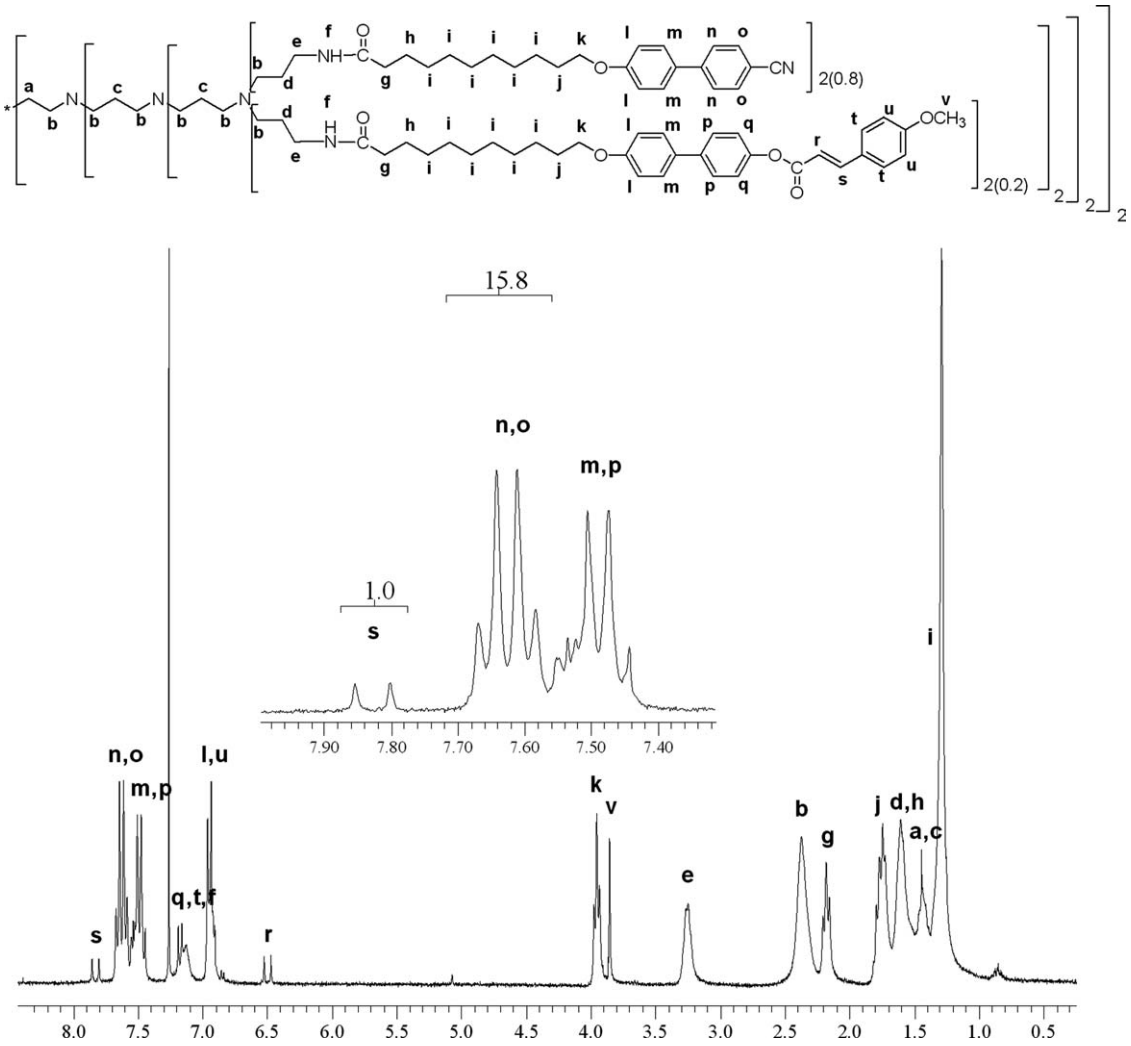


**FIGURE 3** $^{1}$H NMR spectra for [**5**] and peak integration for the calculation of the comonomer composition.

GPC analysis of the dendrimers was performed using as eluent dichloromethane with a 1% v/v of triethylamine to improve the elution of the PPI-derived dendrimers through the column and try to avoid partial adsorption processes due to the amine groups, which lead to high polydispersity values.[36] In general, PI values were low (between 1.2 and 1.08), but the molecular weight was overestimated in all cases.

MALDI-TOF mass spectrometry enabled us to ascertain the extent of substitution at the periphery. For the homodendrimers [**1**] and [**3**], only the parent peak was observed, indicating that all 16 amine end groups of PPI had been modified. The mass spectra of the codendrimers [**4**]–[**7**] showed several peaks, indicating that the material consisted of mixtures of fully functionalized dendrimers (16 in total)

**TABLE 1** Comparative Data for the Calculated Cinnamate Contents (mol %) in Dendrimers from $^{1}$H NMR or UV–vis Spectra, UV–vis Data in Chloroform Solution, and GPC Data Analysis

| Dendrimers | Theoretical Values | $^{1}$H NMR | UV–vis | $\lambda_{max}$ (nm) | $M_w$ | $M_n$ | PI |
|---|---|---|---|---|---|---|---|
| [**1**] | – | – | – | 299 | 11,554 | 10,679 | 1.08 |
| [**3**] | 100 | – | – | 264, 367 | 11,838 | 9,905 | 1.20 |
| [**4**] | 10 | 9 | –[a] | 298 | 11,890 | 10,962 | 1.08 |
| [**5**] | 20 | 20 | –[a] | 298 | 11,580 | 10,768 | 1.07 |
| [**6**] | 10 | 7 | 9 | 297, 368 | 11,549 | 10,595 | 1.09 |
| [**7**] | 20 | 18 | 17 | 294, 367 | 11,624 | 10,378 | 1.12 |

[a] Not determined because of partial overlap of the absorption bands from cyanobiphenyl and cinnamate units.

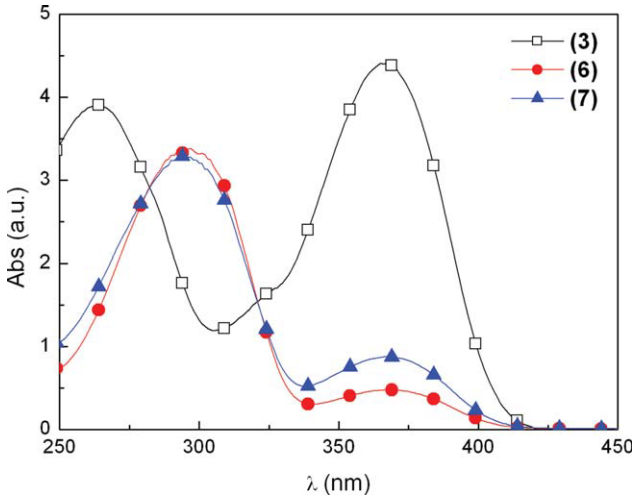


**FIGURE 4** UV–vis spectra in chloroform solution of the 4-(*N,N*-dimethylamino)cinnamate-containing dendrimers. [Color figure can be viewed in the online issue, which is available at wileyonlinelibrary.com.]

but with different numbers of cinnamate or cyanobiphenyl monomers (Table 2 and Fig. 5). Assuming that all the species have the same response to the mass detector, we can assess the relative abundance of the different species from the intensities of the peaks.[36] Correlation of the calculated weights of the possible structures with the peaks observed in the spectrum allowed us to determine the molecular composition. As an example, codendrimer [**4**] essentially contained 29% of molecules with 14 CNB units and two cinnamate units, and 39% of molecules with 15 CNB units and one cinnamate monomer, together with minor amounts of other dendrimeric compositions.

### Thermal Properties of the Monomers

Pentafluorophenyl ester monomers were characterized by polarizing optical microscopy (POM) and differential scanning calorimetry (DSC). Phase transitions and enthalpy values are collected in Table 3.

**CNB** is a liquid crystal with two monotropic mesophases. The compound is a crystalline solid that melts directly on heating to the isotropic liquid. However, on cooling, a schlieren texture develops at 41 °C, and this is typical of a nematic mesophase. On further cooling, the phase transforms into a SmA phase, with homeotropic and fan-shaped textures observed at 36 °C.

Cinnamate monomers have higher transition temperatures as consequence of their extended aromatic core. $\mathbf{M_{NMe2}}$ does not show liquid crystalline properties. In contrast, $\mathbf{M_{OMe}}$ is more rigid and conjugated than $\mathbf{M_{NMe2}}$, and this allows stabilization of a SmA phase between 110 and 166 °C and a nematic mesophase up to 204 °C. The SmA mesophase has a strong tendency toward homeotropic alignment [Fig. 6(a)]. We observed poor reproducibility in DSC cycles, which has been attributed to partial decomposition of the pentafluorophenyl ester and the conjugated cinnamate ester on heating at high temperatures.

### Thermal Properties of the Dendrimers

Thermogravimetric analysis (TGA) of the dendrimers showed the excellent stability toward volatile decomposition, with onset temperatures for weight loss above 360 °C and a first derivative of the weight loss (DTGA) over 396 °C (Table 4). It is known that dendrimers tend to retain small molecules within their inner cavity, and, for this reason, the dendrimers were dried at 80 °C under vacuum for 2 days before performing the analysis. It is interesting to note that these cinnamate dendrimers are much more stable in TGA than similar cyanoazobenzene-containing dendrimers.[32]

The phase behavior of the dendrimers was investigated by DSC and POM. The transition temperatures and enthalpies determined both on heating and cooling are summarized in Table 4. All dendrimers were liquid crystalline except for [**3**], which lacks of mesomorphic peripheral units, and this again provides evidence of the influence of the ethylene spacer and the terminal group of the cinnamate units on the mesomorphic properties of the final dendritic macromolecule. Compounds [**2**] and [**4**]–[**7**] display at the POM focal-conic textures that coexist with a homeotropic texture and these are characteristic of a SmA mesophase [Fig. 6(b–d)]. In particular, Compounds [**6**] and [**7**] show a high tendency toward

**TABLE 2** MALDI-TOF MS Data and Peak Assignments

| Dendrimers | Calculated Mass | MS Peaks (*m/z*) | Peak Relative Abundance (%) | *x*/*y*[a] |
|---|---|---|---|---|
| [**1**] | 7470.4 | 7470.4 | 100 | 16/0 |
| [**3**] | 10802.5 | 10803 | 100 | 16/0 |
| [**4**] | 7772.7[b] | 8076.0 | 3 | 12/4 |
| | | 7924.5 | 12 | 13/3 |
| | | 7773.4 | 29 | 14/2 |
| | | 7622.3 | 39 | 15/1 |
| | | 7471.3 | 17 | 16/0 |
| [**5**] | 7923.9[c] | 8227.7 | 8 | 11/5 |
| | | 8076.6 | 19 | 12/4 |
| | | 7925.5 | 31 | 13/3 |
| | | 7773.5 | 28 | 14/2 |
| | | 7622.4 | 14 | 15/1 |
| [**6**] | 7886.9[b] | 8304.9 | 3 | 12/4 |
| | | 8095.8 | 10 | 13/3 |
| | | 7888.7 | 30 | 14/2 |
| | | 7679.6 | 39 | 15/1 |
| | | 7471.4 | 18 | 16/0 |
| [**7**] | 8095.2[c] | 8514.1 | 8 | 11/5 |
| | | 8304.9 | 21 | 12/4 |
| | | 8096.8 | 28 | 13/3 |
| | | 7887.7 | 29 | 14/2 |
| | | 7678.6 | 14 | 15/1 |

[a] Number of cyanobiphenyl units (*x*) and cinnamate units (*y*) in a molecule, given in relation to the 16 free amino groups of PPI.
[b] Calculated molecular weight of a codendrimer with $x/y = 14/2$.
[c] Calculated molecular weight of a codendrimer with $x/y = 13/3$.

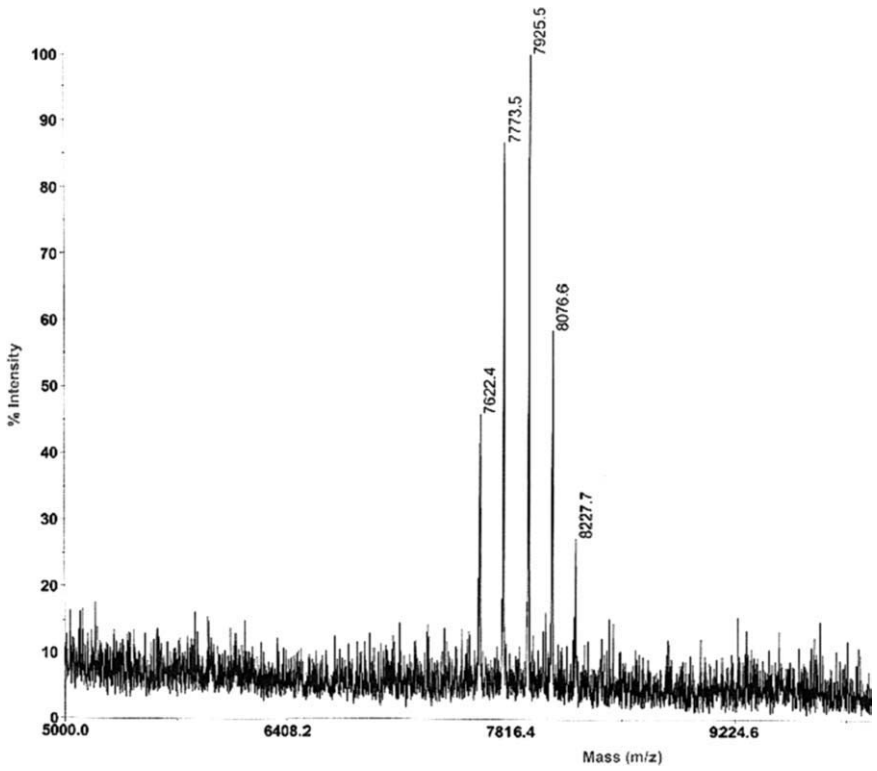


**FIGURE 5** MALDI-TOF MS of codendrimer [**5**] showing the molecular composition.

homeotropic orientation. In general, these cinnamate dendrimers have higher tendency toward crystallization than analogous cyanoazobenzene dendrimers.[32]

Dendrimers with 4-methoxycinnamate-derived monomers [**2**], [**4**], and [**5**] exhibit the mesophase SmA in a broad range. Codendrimers [**4**] and [**5**] have lower isotropization temperatures than the corresponding homodendrimer [**2**], as well as broader mesophase interval. On cooling, from the SmA mesophase, the crystallization is observed for all the compounds, at 125 °C for [**2**] and at about 40 °C for [**4**] and [**5**]. Also, the three compounds showed low reproducibility in the DSC cycles if the isotropization point was reached. This is probably associated with a thermal reaction of the biphenyl 4-methoxycinnamate unit, in a similar way to the found for the cinnamate monomer $\mathbf{M_{OMe}}$. As an example, homodendrimer [**2**] was a crystalline material that melted at 157 °C and exhibited a SmA mesophase up to 239 °C. DSC curves were not reproducible in subsequent cycles, and, on cooling, the isotropic liquid a Schlieren texture could be observed at the POM, which may belong to the thermal behavior of a mixture containing decomposed species. Nevertheless, the transitions and associated enthalpies are reproducible as far as thermally induced reactions of cinnamates are avoided, that is, isotropization is not reached. In this case, DSC traces recorded on heating show several endotherms and even exotherms, which are associated to melting of different crystalline forms. From our experience, this is not uncommon for dendrimers and dendrons.

**TABLE 3** Phase Transitions and Thermodynamic Data for the Monomers

| Monomers | Transition | $T$ (°C) | $\Delta H$ (kJ mol$^{-1}$) |
|---|---|---|---|
| **CNB**[a] | Cr-I | 73 | 55.8 |
| | I-N | 41 | 0.5 |
| | N-SmA | 36 | 0.5 |
| | SmA-Cr | 26 | 30.3 |
| $\mathbf{M_{OMe}}$ | Cr-SmA | 110 | 38.3 |
| | SmA-N | 166 | –[b] |
| | N-I | 204 | 1.3 |
| $\mathbf{M_{NMe2}}$ | Cr-I | 127 | 65.9 |

[a] Pentafluorophenyl 11-[4′-cyano-4-biphenyloxy]undecanoate.
[b] Transition only observed by polarizing optical microscopy.

As a consequence of the more flexible structure of the cinnamate, dendrimers with 4-(*N,N*-dimethylamino)cinnamate units [**6**] and [**7**] show the lowest isotropization points and consequently narrower mesophase interval than the methoxy counterparts. The decrease of the isotropization temperatures also restricts thermally induced reactions that are not observed from the DSC traces. Both compounds crystallize on cooling; however, the DSC thermogram of [**7**] show, in the second heating cycle, a glass transition at 29 °C pointing to a lesser extent of crystalline degree. On further heating above the $T_g$, several overlapped melting peaks between 97 and 130 °C coexist with the mesophase. On cooling, the SmA mesphase is stable between 127 and 71 °C when crystallization occurs.

### Photoinduced Optical Anisotropy and Its Thermal Amplification

The investigated dendrimers are functionalized with two units: photosensitive cinnamoyl and mesogenic cyanobiphenyl. The irradiation with LPUV light leads to the

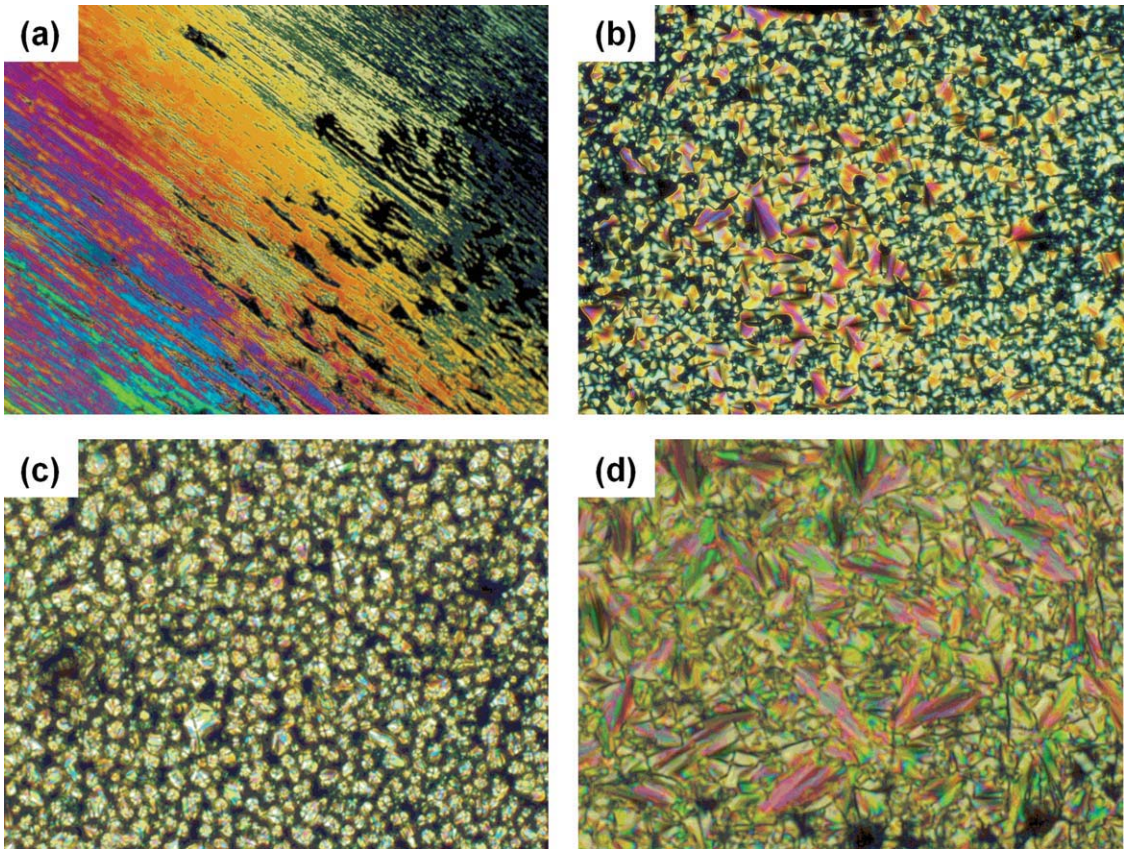


**FIGURE 6** POM microphotographs of $\mathbf{M_{OMe}}$ at 112 °C after rubbing stress (a), [**2**] at 179 °C (b), [**4**] at 135 °C (c), and [**7**] at 120 °C (d).

generation of optical anisotropy as result of axis-selective [2+2] cycloaddition, as well as *E–Z* photoisomerization.[37,38] (Fig. 7). As shown for cinnamate containing LC side chain polymers, annealing in the LC phase may lead to bulk alignment causing a significant amplification of the initially photoinduced optical anisotropy generated in the amorphous state.[14,24,39,40]

The cinnamate codendrimers [**4**]–[**7**] were spin coated onto quartz glass plates and irradiated with LP UV light. The film forming properties, using good solvents like 1,1,2-trichloroethane or THF, were rather poor, always showing some scattering. These could be related to their liquid crystallinity and the tendency of crystallization rather than to form an amorphous glassy film at room temperature. The thicknesses of the films were between 25 and 35 nm. Apart from the structural characteristics of the materials, it is known that there are a lot of factors, which may have an impact on the amplification of the photoinduced anisotropy. We checked for various ones: irradiation wavelength (we chose 324 and 364 nm as they were in the absorption band of the 4-methoxycinnamate dendrimers or the 4-(*N,N*-dimethylamino)cinnamate dendrimers, respectively), irradiation time (from 10 s to 30 min), temperature of annealing (from 5 °C above the melting point and 5 °C below the clearing point), and thickness of the films.

A typical experiment for the codendrimers containing the 4-methoxycinnamate (Fig. 8) and 4-(*N,N*-dimethylamino)cinnamate units (Fig. 9) is described below. A thin films series of

**TABLE 4** Thermal Stability and Thermodynamic Data for the Dendrimers

| Dendrimers | TGA/ $T_{onset}$ (°C)[a] | Thermal Transitions (°C) [$\Delta H$ (J g$^{-1}$)][b] |
|---|---|---|
| [**1**][32] | 367 | Cr 104 [49.8] SmA 125 [9.3] I |
| | | I 121 [8.8] SmA 43 [23.0] Cr |
| [**2**] | 361 | Cr 158 [40.9] SmA 239 [–] I[c] |
| | | SmA 125 [20.25] Cr |
| [**3**] | 368 | Cr 142 [38.2] I |
| | | I 130 [37.1] Cr |
| [**4**] | 371 | Cr 99 [40.0] SmA 149 [–] I[c] |
| | | SmA 37 [19.3] Cr |
| [**5**] | 361 | Cr 95 [21.4] SmA 174 [–] I[c] |
| | | SmA 43 [18.3] Cr |
| [**6**] | 362 | Cr 98 [30.1] SmA 128 [8.4] I |
| | | I 124 [8.2] SmA 47 [21.9] Cr |
| [**7**] | 364 | g 29 Cr 97 [–] SmA 130 [–][d] I |
| | | I 126 [8.5] SmA 71 [23.0] Cr |

[a] Decomposition temperature determined by thermogravimetric analysis (TGA).
[b] Thermal transitions determined by DSC from the peak maximum upon heating and cooling at 10 °C min$^{-1}$.
[c] Thermal reaction was observed associated to the isotropization. Data on cooling is given for a sample heated just above the the SmA-I transition.
[d] Several overlapped peaks are observed in the 97–130 °C interval.

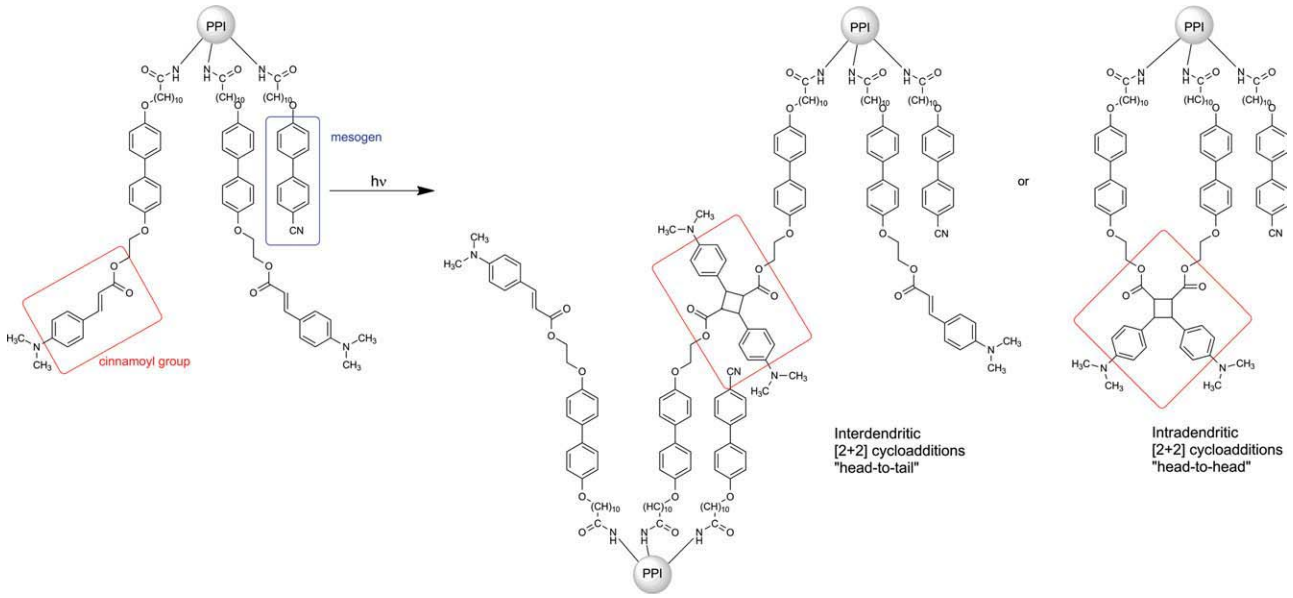


**FIGURE 7** [2+2] Cycloaddition of 4-(*N,N*-dimethylamino)cinnamate PPI dendrimers [**6**] and [**7**] under irradiation with UV light ($\lambda$ = 364/365 nm). [Color figure can be viewed in the online issue, which is available at wileyonlinelibrary.com.]

[**4**] and [**5**], with 10 and 20 mol % of 4-methoxycinnamate, were irradiated at 324 nm from 10 s to 30 min. The samples were stored for 24 h before further investigations. The absorption change for the irradiation time below 1 min was barely observed. For longer exposure time, with a photoconversion of cinnamate esters groups above 10%, the photoinduced anisotropy was noticeable by UV–vis spectroscopy. A decrease of angular absorbance is observed in the direction of the electric field vector, whereas in the direction perpendicular to it remains constant. All films were subsequently annealed in the SmA mesophase (105 °C, 48 h) and a significant drop in the absorbance was observed in the whole spectrum together with a slight red shift of the band. This indicates the out-of-plane orientation of the mesogenic side groups (Fig. 10) and *J*-aggregation.[14] In contrast to glassy LC polymers, we could not find a planar amplification; the tendency of homeotropic alignment of the smectic dendrimers dominates. Interestingly and in contrast to the polymers, the maximum of absorbance is perpendicular to the electric field vector indicating the alignment by remaining cinnamate groups. The best dichroism after annealing obtained with these samples was 0.1.

The same result was observed for the codendrimers [**6**] and [**7**] (Fig. 9), with 10 and 20 mol % of 4-(*N,N*-dimethylamino)cinnamate units, where the absorption band of the photoactive cinnamate units is separated from that of the mesogen. In that case, irradiation at 364 nm for 6 min led to the

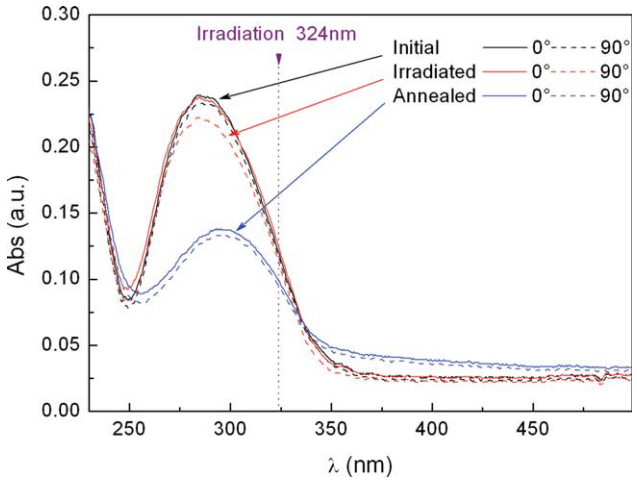


**FIGURE 8** Changes of polarized absorbance spectra in a film of [**4**], under irradiation with linearly polarized light ($\lambda$ = 324 nm, $P$ = 20 mW cm$^{-2}$, $t$ = 3 min). [Color figure can be viewed in the online issue, which is available at wileyonlinelibrary.com.]

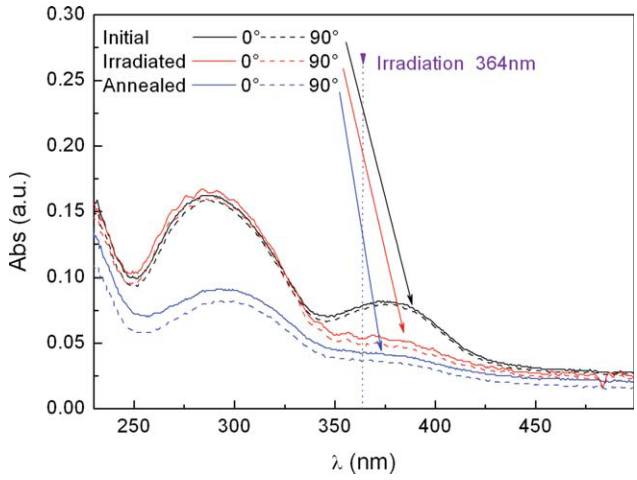


**FIGURE 9** Changes of polarized absorbance spectra in a film of [**7**], under irradiation with linearly polarized light ($\lambda$ = 364 nm, $P$ = 10 mW cm$^{-2}$, $t$ = 6 min). [Color figure can be viewed in the online issue, which is available at wileyonlinelibrary.com.]

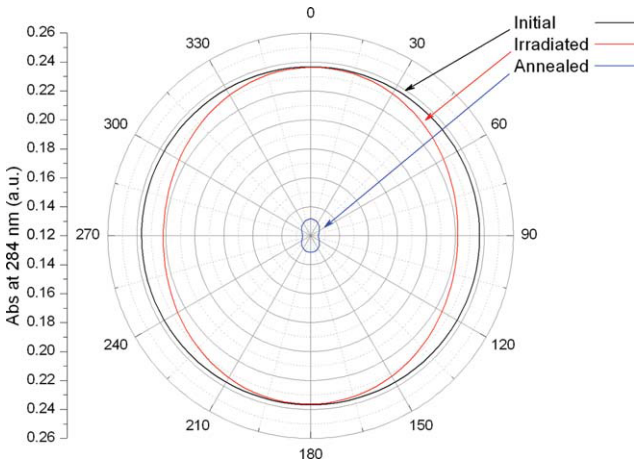


**FIGURE 10** Polar plots of the absorbance of [**4**] at 284 nm of the initial state, after irradiation and annealing process. [Color figure can be viewed in the online issue, which is available at wileyonlinelibrary.com.]

decrease of absorbance of the cinnamate chromophore at 375 nm of 35%, which indicates a photoresponse due to photocrosslinking through [2+2] photocycloaddition. Although, the absorbance at 280 nm corresponding to the cyanobiphenyl unit remained stable. After annealing in the SmA mesophase (125 °C, 48 h), a drop in the absorbance was observed in the full spectrum due to the out-of-plane orientation.

In all cases, the photoinduced anisotropy was decreased or lost after annealing. We believe that the low tendency to form a glassy state is a drawback for the amplification process and our future work in this direction is underway. This work represents a proof of the principle that LC dendrimers functionalized with cinnamate groups could behave similar as side-chain LC cinnamate polymers with the aim of developing novel photoresponsive materials.

## CONCLUSIONS

Cinnamate dendrimers with liquid crystalline properties have been prepared by attaching 4-methoxycinnamate or 4-(*N,N*-dimethylamino)cinnamate units and/or cyanobiphenyl units at the periphery of the third generation PPI dendrimer. Full functionalization of this middle-generation PPI core has been obtained. Thin films of dendrimers are photoactive, and a photoinduced anisotropy is observed, although it could not be amplified by thermal annealing. This preliminary result leads us to conclude that the polymer approach followed in photoresponsive cinnamate side chain liquid crystalline polymers can be translated to cinnamate dendrimers, which, in principle, allow better control of the molecular composition and characterization. LC photoactive cinnamate macromolecules that show clearly differentiated absorption regions for the photoactive unit and the LC unit have been prepared by introducing the 4-(*N,N*-dimethylamino)cinnamate moiety. This objective is of interest to avoid interferences with other chromophores in the irradiation experiments. Further work is in progress to optimize the structure of the photoactive cinnamate unit trying to gain amorphous materials with improved film forming properties.

The authors thank the Gobierno de Aragón (project PI109/09, research group E04), MICINN-Spain and FSE-UE (projects MAT2008-06522-CO2-01 and MAT2009-14636-CO3-01), and UE project (7th FP—THE PEOPLE PROGRAMME. The Marie Curie Actions—ITN, No. 215884-2).

## REFERENCES AND NOTES

**1** Newkome, G. R.; Moorefield, C. N.; Vögtle, F. Dendritic Molecules: Concepts, Syntheses, and Applications; Wiley-VCH: Weinheim, Germany, 1996.

**2** Fréchet, J. M. J.; Tomalia, D. A. Dendrimers and Other Dendritic Polymers; Wiley-VCH: Weinheim, Germany, 2001.

**3** Menjoge, A. R.; Kannan, R. M.; Tomalia, D. A. Drug Discov Today 2010, 15, 171–185.

**4** Astruc, D.; Boisselier, E.; Ornelas, C. Chem Rev 2010, 110, 1857–1959.

**5** Rosen, B. M.; Wilson, C. J.; Wilson, D. A.; Peterca, M.; Imam, M. R.; Percec, V. Chem Rev 2009, 109, 6275–6540.

**6** Zeng, F.; Zimmerman, S. C. Chem Rev 1997, 97, 1681–1712.

**7** Shibaev, V.; Bobrovsky, A.; Boiko, N. Prog PolymSci 2003, 28, 729–836.

**8** Deloncle, R.; Caminade, A. M. J. Photochem Photobiol C-Photochem Rev 2010, 11, 25–45.

**9** Ichimura, K. Chem Rev 2000, 100, 1847–1873.

**10** Natansohn, A.; Rochon, P. Chem Rev 2002, 102, 4139–4175.

**11** Yu, H. F.; Kobayashi, T. Molecules 2010, 15, 570–603.

**12** Meier, J. G.; Ruhmann, R.; Stumpe, J. Macromolecules 2000, 33, 843–850.

**13** Kawatsuki, N.; Matsuyoshi, K.; Yamamoto, T. Macromolecules 2000, 33, 1698–1702.

**14** Kawatsuki, N.; Goto, K.; Kawakami, T.; Yamamoto, T. Macromolecules 2002, 35, 706–713.

**15** Kawatsuki, N.; Tsutsumi, R.; Takatsuka, H.; Sakai, T. Macromolecules 2007, 40, 6355–6360.

**16** Stumpe, J.; Läsker, L.; Fischer, T.; Kostromin, S.; Ruhmann, R. Thin Solid Films 1996, 284, 252–256.

**17** Rosenhauer, R.; Fischer, T.; Czapla, S.; Stumpe, J.; Vinuales, A.; Pinol, M.; Serrano, J. L. Mol Cryst Liq Cryst 2001, 364, 295–304.

**18** Bobrovsky, A.; Boiko, N.; Shibaev, V.; Stumpe, J. J Photochem Photobiol A-Chemistry 2004, 163, 347–358.

**19** Kawatsuki, N.; Takatsuka, H.; Yamamoto, T.; Ono, H. Jpn J Appl Phys 1997, 36, 6464–6469.

**20** Kawatsuki, N.; Suehiro, C.; Yamamoto, T. Macromolecules 1998, 31, 5984–5990.

**21** Kawatsuki, N.; Matsuyoshi, K.; Hayashi, M.; Takatsuka, H.; Yamamoto, T. Chem Mater 2000, 12, 1549–1555.

**22** Gimenez, R.; Millaruelo, M.; Pinol, M.; Serrano, J. L.; Vinuales, A.; Rosenhauer, R.; Fischer, T.; Stumpe, J. Polymer 2005, 46, 9230–9242.

**23** Rosenhauer, R.; Fischer, T.; Stumpe, J.; Gimenez, R.; Pinol, M.; Serrano, J. L.; Vinuales, A.; Broer, D. Macromolecules 2005, 38, 2213–2222.

**24** Rosenhauer, R.; Stumpe, J.; Gimenez, R.; Pinol, M.; Serrano, J. L.; Vinuales, A. Macromol Rapid Commun 2007, 28, 932–936.

**25** Wang, J.; Jia, W.; Zhong, H.; Wu, H.; Li, Y.; Xu, X.; Li, M.; Wei, Y. J. Polym Sci Part A: Polym Chem 2000, 38, 4147–4153.

**26** Ni, Y.; Zheng, S. Chem Mater 2004, 16, 5141–5148.

**27** Boiko, N.; Zhu, X. M.; Bobrovsky, A.; Shibaev, V. Chem Mater 2001, 13, 1447–1452.

**28** Donnio, B.; Buathong, S.; Bury, I.; Guillon, D. Chem Soc Rev 2007, 36, 1495–1513.

**29** Marcos, M.; Martin-Rapun, R.; Omenat, A.; Serrano, J. L. Chem Soc Rev 2007, 36, 1889–1901.

**30** Baars, M.; Sontjens, S. H. M.; Fischer, H. M.; Peerlings, H. W. I.; Meijer, E. W. Chem Eur J 1998, 4, 2456–2466.

**31** Donnio, B.; Barbera, J.; Gimenez, R.; Guillon, D.; Marcos, M.; Serrano, J. L. Macromolecules 2002, 35, 370–381.

**32** Alcalá, R.; Giménez, R.; Oriol, L.; Piñol, M.; Serrano, J. L.; Villacampa, B.; Viñuales, A. I. Chem Mater 2007, 19, 235–246.

**33** Kawatsuki, N.; Sakashita, S.; Takatani, K.; Yamamoto, T.; Sangen, O. Macromol Chem Phys 1996, 197, 1919–1935.

**34** Schenning, A.; Elissen-Roman, C.; Weener, J. W.; Baars, M.; van der Gaast, S. J.; Meijer, E. W. J Am Chem Soc 1998, 120, 8199–8208.

**35** Pastor, L.; Barbera, J.; McKenna, M.; Marcos, M.; Martin-Rapun, R.; Serrano, J. L.; Luckhurst, G. R.; Mainal, A. Macromolecules 2004, 37, 9386–9394.

**36** Bu, L.; Nonidez, W. K.; Mays, J. W.; Tan, N. B. Macromolecules 2000, 33, 4445–4452.

**37** Ichimura, K.; Akita, Y.; Akiyama, H.; Kudo, K.; Hayashi, Y. Macromolecules 1997, 30, 903–911.

**38** Chae, B.; Lee, S. W.; Ree, M.; Jung, Y. M.; Kim, S. B. Langmuir 2003, 19, 687–695.

**39** Kawatsuki, N.; Yamashita, A.; Fujii, Y.; Kitamura, C.; Yoneda, A. Macromolecules 2008, 41, 9715–9721.

**40** Rosenhauer, R.; Stumpe, J.; Gimenez, R.; Piñol, M.; Serrano, J. L.; Viñuales, A.; Broer, D. Macromolecules 2011, 44, 1438–1449.